

Color-selecting reflectors inspired from biological periodic multilayer structures

O. Deparis, C. Vandembem, M. Rassart, V. L. Welch, J.-P. Vigneron

Solid State Physics Lab., Physics Dept., Facultés Universitaires Notre-Dame de la Paix, B-5000 Namur, Belgium

<http://www.fundp.ac.be/facultes/sciences/departements/physique/recherche/centres/lps/>

Abstract: We propose a semi-infinite 1-D photonic crystal approach for designing artificial reflectors which aim to reproduce color changes with the angle of incidence found in biological periodic multilayer templates. We show that both the dominant reflected wavelength and the photonic bandgap can be predicted and that these predictions agree with exact calculations of reflectance spectra for a finite multilayer structure. In order to help the designer, the concept of spectral richness of angle-tuned color-selecting reflectors is introduced and color changes with angle are displayed in a chromaticity diagram. The usefulness of the photonic crystal approach is demonstrated by modelling a biological template (found in the cuticle of *Chrysochora vittata* beetle) and by designing a bio-inspired artificial reflector which reproduces the visual aspect of the template. The bio-inspired novel aspect of the design relies on the strong unbalance between the thicknesses of the two layers forming the unit cell.

©2006 Optical Society of America

OCIS codes: 260.2110 Electromagnetic theory, 330.1690 Color, 260.3160 Interference, 160.4890 Organic materials.

References and Links

1. Serge Berthier, *Les couleurs des Papillons, ou l'impérative beauté : propriétés optiques des ailes de papillons* (Springer-Verlag, Paris, 2000).
2. S. Kinoshita and S. Yoshioka (Eds), *Structural Colors in Biological Systems: Principles and Applications* (Osaka Univ. Press, Osaka, 2005).
3. J.-P. Vigneron, M. Rassart, C. Vandembem, V. Lousse, O. Deparis, L. P. Biró, D. Dedouaire, A. Cornet, P. Defrance, "Spectral filtering of visible light by the cuticle of metallic woodboring beetles and microfabrication of a matching bioinspired material," to be published in Phys. Rev. E, 2006.
4. European NEST STREP BioPhot project (contract n°12915).
5. P. Yeh, *Optical waves in layered media*, 2nd Ed. (John Wiley & Sons, Hoboken N. J., 2005).
6. A. Dereux, J.-P. Vigneron, Ph. Lambin, A. A. Lucas, "Polaritons in semiconductor multilayered materials," Phys. Rev. B **38**, 5438 (1988).
7. V. L. Welch, J.-P. Vigneron, A. R. Parker, "The cause of coloration in the ctenophore *Beroë cucumis*," Current Biology, **15**, R985 (2005).
8. J.P. Vigneron, J.-F. Colomer, N. Vigneron and V. Lousse, "Natural layer-by-layer photonic structure in the squamae of *Hoplia coerulea* (Coleoptera)," Phys. Rev. E **72**, 061904 (2005).
9. B. Gralak, G. Tayeb, S. Enoch, "Morpho butterflies wings color modeled with lamellar grating theory," Opt. Express **9**, 567 (2001).

1. Introduction

In nature, e.g., among insects, it is frequent to find periodic multilayer structures which produce vivid and metallic colors upon reflection of light by the surface [1, 2]. The metallic finish of the surface comes from the strict specularity of the light reflection whereas the vivid coloration results from the sharp filtering reflectance. Also, an interesting feature is the fact that the hue of the reflection changes as the angle of incidence is changed from normal to grazing. These features are observed, e.g., in the Buprestidae (Coleoptera) family of insects, among which *Chrysochora vittata* is a typical example. On the hard protective cover (elytron)

which hides its wings, a metallic green color is displayed which turns to blue under large angles; on the other side, its abdomen appears red under normal incidence and shows a bluish green at grazing incidences (Fig. 1). The origin of these colors were found to be in the detailed structure of the exocuticle, which consists of a periodic air-chitin multilayer stack acting as an angle-dependent spectrally selective reflector for visible light [3]. The remarkable characteristic of this naturally optimized 1-D photonic crystal lies in the fact that regularly spaced thin air layers act as a periodic perturbation of the otherwise homogenous bulk chitin material (refractive index close to 1.56). Therefore the colors produced by photonic bandgap-type reflection depend on the distance separating the perturbing layers, but do not depend on the material which fills them. By exploiting the robustness of this thin-layer design, the changing colors of *Chrysochroa vittata* were “copied” into a bio-inspired artificial reflector, with thin metal layers acting as periodic perturbation of a dielectric [3].

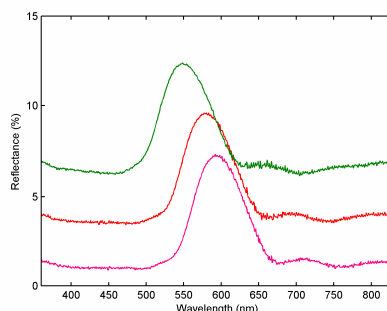


Fig. 1 Reflectance spectra measured on a biological sample (cuticle of *Chrysochroa vittata* beetle - ventral side) at angles of incidence equal to 20° (magenta line), 30° (red line) and 45° (green line) using TE-polarized light. A metallic mirror was used as reference in a variable-angle specular reflectance measurement setup. Note the shift of the dominant reflected wavelength towards the shorter wavelengths as the angle of incidence was increased.

Our purpose here is to exploit more systematically the photonic crystal design approach for the fabrication of bio-inspired color-selecting reflectors. Such a task is part of a more general and ambitious goal, which is to operate a significant technology transfer from natural biology to synthetic materials science [4]. In the case of natural multilayer structures, we find combinations of materials and geometrical parameters which have resulted from millions of years of adaptation, and which can provide us with an inexhaustible source of both speculation and inspiration. In the case of multilayer artificial structures, materials can be chosen from among a large variety of candidates, such as dielectrics, semiconductors, metals and polymers. However, one has to select a combination of materials (here two) which is compatible with layer-by-layer fabrication requirements. Although the choice for these is, again, vast (cf. e.g., sputtering processes), the material parameters, such as the refractive indexes, can not be varied arbitrarily. By contrast, the geometrical parameters, such as the layer thicknesses, can be varied continuously within a large range. The control of layer thicknesses is easy in the usual fabrication processes and provides us with great design flexibility. Biological structures, by contrast, whilst they vary hugely in their morphologies [1, 2], are severely restricted in their refractive indices and, hence, optical layer thicknesses: indeed, all materials found in biological color-producing structures have refractive indices between 1.00 (air) and 1.83 (guanine). By exploiting the wide range of morphologies found in biological color-producing structures and combining these with materials chosen from the vast range at our disposal, not only can we harness the best of natural and artificial designs, but we can create structures to fulfil functions and suit situations above and beyond those found naturally.

2. Photonic crystal design approach

The choice of relevant features of the reflectance spectrum is the first step of the design of color-selecting reflectors. If the design is kept simple, the reflectance spectrum exhibits a

single peak in the visible range as the angle of incidence is varied and the changing colors are determined by the shift of the dominant reflected wavelength. The dominant reflected wavelength is considered as the first design element. The spectral width of the reflectance peak, which determines the purity of the color, is related to the (not complete) photonic bandgap associated with the one-dimensional periodic multilayer structure. The normalized width of the photonic bandgap is considered as a second design element. Using these two elements, the main features of the reflectance can be predicted by simple formulae.

The reflectors we aim to design are inspired from biological periodic multilayer structures, for which the refractive index contrast is always low (~ 1.8 at maximum). In our approach, we first replace the stack made by the periodic arrangement of a finite number of layers by a semi-infinite effective metamaterial of average index \bar{n} , which is determined by considering a period of two layers in the frame of a “long wavelength approximation”. In doing that we must distinguish two extreme cases: the electric field of the incident electromagnetic wave is parallel to the layer interfaces or is perpendicular. The former case is valid for transverse-electric (TE) waves at any angle of incidence and is a good approximation for transverse-magnetic (TM) waves at low angles (near normal incidence); the later case is approximately valid for TM waves at large angles (near grazing incidence). Neglecting retardation effects, layers can be seen as a parallel or serial assembly of capacitances, respectively. Using the rules of capacitances, the average refractive index can be expressed by

$$\bar{n}_{\parallel} = \left(\frac{n_1^2 d_1 + n_2^2 d_2}{d_1 + d_2} \right)^{1/2} = n_1 \left(\frac{1 + rc^2}{1 + r} \right)^{1/2} \quad (1-a)$$

and

$$\bar{n}_{\perp} = \left(\frac{d_1/n_1^2 + d_2/n_2^2}{d_1 + d_2} \right)^{-1/2} = n_1 \left(\frac{1 + r}{1 + r/c^2} \right)^{1/2} \quad (1-b)$$

respectively. In eq. (1), we have introduced the following design parameters: the layer thickness ratio $r = d_2/d_1$, the refractive index of the least refringent layer n_1 (hereafter called the basic index), and the index contrast $c = n_2/n_1 = (\epsilon_2/\epsilon_1)^{1/2}$. For simplicity we consider lossless dielectric materials (n is real) and we neglect index dispersion in the wavelength range of interest, which is a reasonable approximation for the materials under study. Note that Eq. (1) shows that anisotropy is produced by the bi-layer arrangement even if the layer indexes are isotropic [5].

The next step is to consider the refractive index contrast as a weak periodic perturbation which defines a semi-infinite 1-D photonic crystal along the normal to the layers (z axis). By expressing the conservation of the lateral wavevector at the interface between the incident medium (air) and the photonic crystal, one can obtain the band-gap formation condition [3]:

$$k_z = m \frac{\pi}{a} = \sqrt{\left[\bar{n} \frac{\omega}{c} \right]^2 - k_y^2} \quad (2)$$

where ω is the angular frequency, c is the light velocity in vacuum, m is an integer, θ is the angle of incidence, $a = d_1 + d_2$ is the period, $k_y = \omega/c \times \sin \theta$ is the lateral wavevector, $k_z = m\pi/a$ is the normal wavevector which can take only discrete values according to Bloch's theorem. From Eq. (2), it is straightforward to determine the dominant reflected wavelength as a function of the angle of incidence:

$$\lambda_{\theta} = \frac{2a\sqrt{\bar{n}^2 - \sin^2 \theta}}{m} \quad (3)$$

For an infinite number of periods, total reflectance will appear at these wavelengths, assuming a weak refractive index contrast. This very general formula shows that the reflectance peak experiences a blue shift as the angle of incidence increases: this is the effect we want to exploit for the realization of bio-inspired color-selecting reflectors.

In order to compare designs with different geometrical and material parameters, it is convenient to fix the value of the dominant reflected wavelength at normal incidence and to scale the physical dimensions of the structure accordingly. Actually, it is only necessary to scale e.g. the thickness of the least refringent layer, since the other dimensions follow from $d_2 = rd_1$ and $a = d_1(1+r)$. By substituting Eq. (1) into Eq. (3) with $\theta = 0$, the thickness of the least refringent layer is deduced:

$$d_{\parallel} = m \frac{\lambda_{\theta=0}}{2n_1} \left[(1+rc^2)(1+r) \right]^{1/2} \quad (4-a)$$

or

$$d_{\perp} = m \frac{\lambda_{\theta=0}}{2n_1} \left[(1+r/c^2)(1+r)^3 \right]^{1/2} \quad (4-b)$$

depending on the orientation of the incident electric field with respect to the layer interfaces. In Eq. (4), $\lambda_{\theta=0} = 2a\bar{n}/m$ is the dominant reflected wavelength at normal incidence. Now, different designs can be compared on the basis of the ‘‘spectral richness’’, which we define by the dimensionless quantity:

$$\Theta_{\parallel} = \frac{\lambda_{\theta\parallel}}{\lambda_{\theta=0}} = \left[1 - \frac{1+r}{1+rc^2} \frac{\sin^2 \theta}{n_1^2} \right]^{1/2} \quad (5-a)$$

or

$$\Theta_{\perp} = \frac{\lambda_{\theta\perp}}{\lambda_{\theta=0}} = \left[1 - \frac{1+r/c^2}{1+r} \frac{\sin^2 \theta}{n_1^2} \right]^{1/2}. \quad (5-b)$$

This quantity is independent of the absolute physical dimensions of the structure. By multiplying it with the chosen value of the dominant reflected wavelength at normal incidence, one obtains the range of wavelengths that is spanned by the dominant reflected wavelength as the angle is varied.

From the point of view of spectral selectivity, different designs can be compared on the basis of the pseudo (not complete) bandgap of the 1-D photonic crystal. By expanding the periodic dielectric function ε in Fourier series, one can obtain a closed-form expression for the normalized bandgap width at normal incidence:

$$\Delta = \frac{\Delta\omega_{gap}}{\omega_0} = \frac{\varepsilon^{(1)} + \varepsilon^{(-1)}}{\varepsilon^{(0)}} = \frac{2}{\pi} \frac{(1+r)(1-c^2) \sin\left(\frac{\pi}{1+r}\right)}{1+rc^2}. \quad (6)$$

3. Predictions of the photonic crystal design approach

The air/chitin bio-structure under consideration was actually found in the cuticle of *Chrysochroa vittata*, a buprestid beetle [3]. Measurements of reflectance spectra of cuticle samples showed that the dominant wavelength under normal incidence was located around 640 nm [3]. For the sake of comparison, we took $\lambda_{\theta=0}$ equal to 640 nm in all calculations. Also we carried out calculations for TE waves so that the same expression of the average index (eq. 1-a) could be used for all angles of incidence. The basic index and the index contrast of the bio-structure were $n_1 = 1.00$ (air) and $c = 1.56$ [2]. For the artificial structure, we took SiO₂ and TiO₂ as the low-index ($n_1 = 1.50$) and high-index ($n_2 = 2.70$) materials, respectively. This choice was somewhat arbitrary but it had the advantage of compatibility with usual layer-by-layer fabrication techniques. Both the basic index and the index contrast ($c = 1.8$) of the artificial structure were higher than those of the bio-structure. The spectral richness (at angles varying from 0° to 80°) and the photonic bandgap (at 0° incidence) were calculated using to Eq. (5) and Eq. (6) respectively for the bio-structure (Fig. 2) and for the artificial structure (Fig. 3) as functions of the ratio between layer thicknesses. The layer thicknesses were scaled according to Eq. (4) in order to keep $\lambda_{\theta=0}$ constant (=640 nm) as the ratio was varied. In terms of wavelengths, a spectral richness of 0.7 corresponded to a shift of the dominant reflected wavelength down to 640×0.7=448 nm. The results of Figs. 2 and 3

revealed that the thinner the high-index layer (the smaller the value of r), the higher the spectral richness, i.e. the larger the blue-shift of the dominant reflected wavelength with increasing angle of incidence. Also, a stronger unbalance between layer thicknesses ($r \gg 1$ or $r \ll 1$) led to a narrower bandgap, i.e., a higher spectral selectivity.

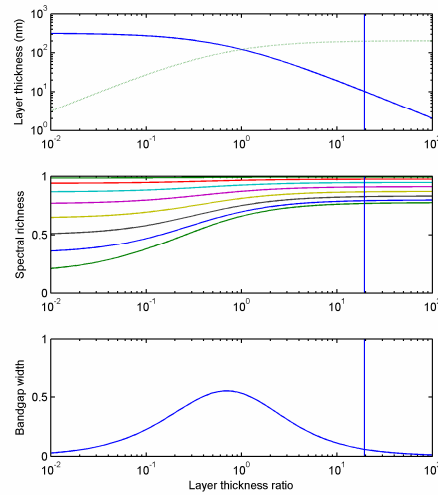


Fig. 2. Layer thicknesses (top graph: solid and dotted lines correspond to low-index layer thickness d_1 and high-index layer thickness d_2 , respectively), spectral richness (middle graph) and bandgap normalized width at 0° incidence (bottom graph) as functions of layer thickness ratio in the case of an air/chitin photonic crystal ($n_1 = 1.0$, $n_2 = 1.56$). The spectral richness was calculated at angles of incidence increasing from 0° to 80° by steps of 10° . Vertical lines correspond to a structure made of 10-nm thick air layers and 194-nm thick chitin layers. All calculations were done for TE polarization.

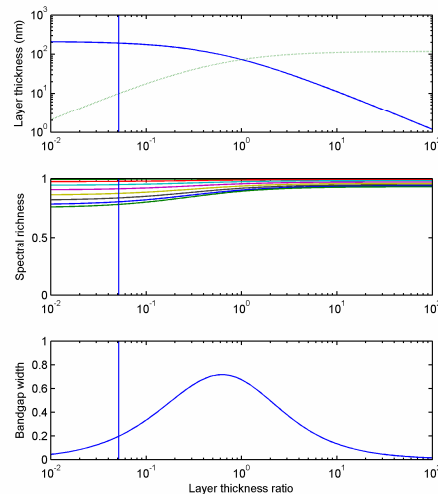


Fig. 3. Layer thicknesses (top graph: solid and dotted lines correspond to low-index layer thickness d_1 and high-index layer thickness d_2 , respectively), spectral richness (middle graph) and normalized bandgap width at 0° incidence (bottom graph) as functions of layer thickness ratio in the case of a $\text{SiO}_2/\text{TiO}_2$ photonic crystal ($n_1 = 1.5$, $n_2 = 2.7$). The spectral richness was calculated at angles of incidence increasing from 0° to 80° by steps of 10° . Vertical lines correspond to a structure made of 10-nm thick TiO_2 layers and 194-nm thick SiO_2 layers. All calculations were done for TE polarization.

Dependencies of the spectral richness (at 60° incidence) and of the photonic bandgap on the layer thickness ratio were calculated for various refractive index contrasts and different values of the basic index (Fig. 4). The results of Fig. 4 revealed that the smaller the basic index and/or the index contrast, the larger the spectral richness. Also, the width of the photonic bandgap decreased with decreasing index contrast, as expected.

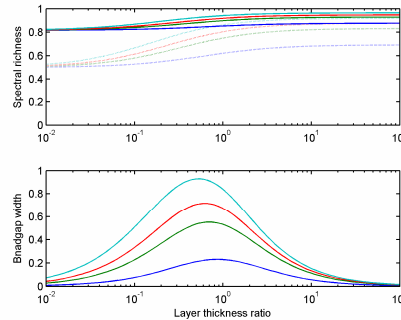


Fig. 4. Spectral richness at an angle of incidence of 60° (top graph) and normalized bandgap width at 0° incidence (bottom graph) as functions of layer thickness ratio in the case of photonic crystal structures with two different values of the basic index (dotted lines: $n_1 = 1.0$, solid lines: $n_1 = 1.5$) and various values of index contrast: $c = n_2/n_1 = 1.20$ (blue lines), 1.56 (green lines), 1.80 (red lines), 2.20 (cyan lines). All calculations were done for TE polarization.

4. Validation of the photonic crystal design approach

In order to validate the predictions of the photonic crystal approach, we compared them with rigorous calculations of reflectance spectra of multilayer structures made of a finite number p of periods. Reflectance spectra were calculated by solving exactly Maxwell's equations [6]. The first multilayer structure (Fig. 5) simulated the cuticle of *Chrysochroa vittata* beetle with its actual refractive indexes ($n_1 = 1.0$, $n_2 = 1.56$), layer thicknesses ($d_1 = 10$ nm, $d_2 = 194$ nm) and approximate number of periods ($p = 20$). The second multilayer structure (Fig. 6) simulated an artificial reflector made of SiO₂ and TiO₂ as low- and high-index materials, respectively. The layer thicknesses had the same values as those of the bio-structure but the thin layer was made of the high index material, as opposed to the biological case (cf. discussion in next paragraph). In both cases, excellent agreement was found between values of the dominant reflected wavelengths calculated from Eq. (3) and those extracted from reflectance spectra.

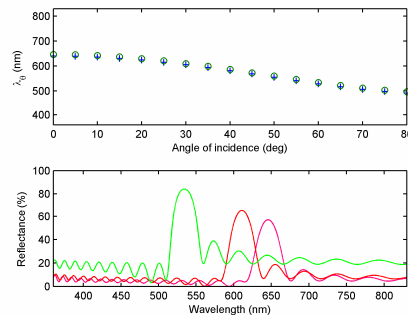


Fig. 5. Dominant reflected wavelength as function of angle of incidence (top graph) and reflectance spectra (bottom graph) at angles of incidence equal to 0° (magenta line), 30° (red line) and 60° (green line) in the case of a periodic multilayer air/chitin structure ($n_1 = 1.0$, $n_2 = 1.56$, $d_1 = 10$ nm, $d_2 = 194$ nm). Values of the dominant reflected wavelengths were calculated by eq. 3 (crosses) or extracted from reflectance spectra (circles). The reflectance spectra were calculated for a structure of 20 periods by solving Maxwell's equations exactly. All calculations were done for TE polarization.

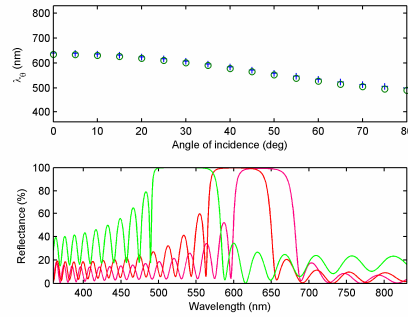


Fig. 6. Dominant reflected wavelength as function of angle of incidence (top graph) and reflectance spectra (bottom graph) at angles of incidence equal to 0° (magenta line), 30° (red line) and 60° (green line) in the case of a periodic multilayer $\text{SiO}_2/\text{TiO}_2$ structure ($n_1 = 1.5$, $n_2 = 2.7$, $d_1 = 194$ nm, $d_2 = 10$ nm). Values of the dominant reflected wavelengths were calculated by eq. 3 (crosses) or extracted from reflectance spectra (circles). The reflectance spectra were calculated for a structure of 20 periods by solving Maxwell's equations exactly. All calculations were done for TE polarization.

5. Bio-inspired designs

In the case of the biological multilayer structure found in *Chrysochroa vittata*'s cuticle, the photonic crystal model predicts a large shift of the dominant reflected wavelength with the angle of incidence, resulting in a spectacular color change from red to green (Fig. 5). The model allows us to explain why the insect is able to achieve both high spectral richness and selectivity (Fig. 2): the key ingredients are unbalanced layer thicknesses ($r = 19.4$), relatively modest index contrast ($n_2/n_1 = 1.56$), small value of the basic index ($n_1 = 1.0$). The latter ingredient of nature's receipt is obtained by supported air spacers [3]. Interestingly, this echoes the situation found in the color-producing structure of the comb-jellyfish *Beroë cucumis* [7], where the organism produces a high spectral richness from a similarly small index contrast. Although a higher spectral richness could have been achieved in *Chrysochroa vittata* with a lower layer thickness ratio, it would have been obtained at the expense of spectral selectivity (larger width of the photonic band gap). The geometry of the natural air/chitin multilayer structure turns out to be remarkably optimized for the spectral filtering of visible light by the insect cuticle. This finding is all the more remarkable when one considers that the insect's cuticle is simultaneously fulfilling the competing and, at times contradictory, demands of numerous other selection pressures. (The cuticle must be comparatively light, yet strong, waterproof etc., as well as fulfilling any optical functions, such as producing the spectral filtering described here). Note that small shifts of the dominant reflected wavelength with the angle of incidence were found in *Hoplia coerculia* (Coleoptera) which displays iridescent blue-violet color [8]. The insect cuticle is made of a multilayer with a very small refractive index contrast ($n_2/n_1 = 1.16$). However, in this case, the basic index is higher than that in *Chrysochroa vittata* and, consistently, the model predicts a lower spectral richness (Fig. 4). In *Hoplia coerculia*, the thickness ratio ($r = 0.33$) is optimized for good spectral selectivity and ensures a sufficiently high value of the reflection coefficient.

In the case of artificial multilayer structures, unless air spacers or porous materials are used, the basic index is higher than the one of the air-chitin structure considered above. As a result of taking e.g., SiO_2 instead of "air" as the low-index material, a penalty on the spectral richness is predicted (Fig. 4). To some extent, it could be compensated for by decreasing the index contrast, i.e., by replacing TiO_2 by another oxide of lower index, but this would be at the expense of decreasing the peak reflectivity. Interestingly, in the case $\text{SiO}_2/\text{TiO}_2$ designs, one can recover a high spectral richness by making the high-index layer (TiO_2) much thinner than the low-index one (SiO_2): this is just the opposite case to *Chrysochroa vittata*. At the same time, a high spectral selectivity can be preserved. The latter case is illustrated by the vertical lines in Fig. 3.

6. Chromaticity diagrams

The visual aspect produced by the structure in reflection under a specified illumination can be quantified in terms of chromaticity coordinates (X,Y,Z) [1, 9]. The latter were calculated from the reflectance spectra $R(\lambda)$ using

$$\begin{aligned} X &= k \int R(\lambda)L(\lambda)x(\lambda)d\lambda \\ Y &= k \int R(\lambda)L(\lambda)y(\lambda)d\lambda \\ Z &= k \int R(\lambda)L(\lambda)z(\lambda)d\lambda \end{aligned} \quad (7)$$

where $L(\lambda)$ is the source spectrum (here D65 illuminant), $x(\lambda)$, $y(\lambda)$ and $z(\lambda)$ are the CIE 1931 color-matching functions, and k is a normalization constant so that $X + Y + Z = 1$. The two independent coordinates (X, Y), which define the chromaticity of the color in a so-called chromaticity diagram, describe a curve as the incidence is varied from normal to grazing. Such a curve allows us to figure out the change in the visual aspect of the object. The curves of the air/chitin structure and the $\text{SiO}_2/\text{TiO}_2$ structure are displayed in Fig. 7 and Fig. 8, respectively. Thanks to its bio-inspired design, the $\text{SiO}_2/\text{TiO}_2$ reflector is able to produce similar colors as the biological template.

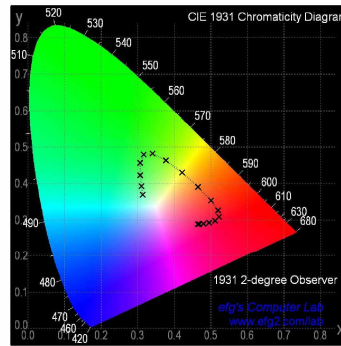


Fig. 7. Evolution of chromaticity coordinates as the angle of incidence is increased from 0° to 80° by steps of 5° in the case of 20-periods air/chitin multilayer structure ($n_1 = 1.0$, $n_2 = 1.56$, $d_1 = 10$ nm, $d_2 = 194$ nm).

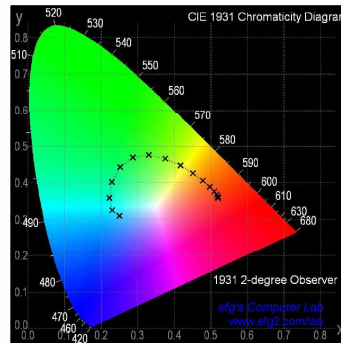


Fig. 8. Evolution of the chromaticity coordinates as the angle of incidence is increased from 0° to 80° by steps of 5° in the case of a 20-periods $\text{SiO}_2/\text{TiO}_2$ multilayer structure ($n_1 = 1.5$, $n_2 = 2.7$, $d_1 = 194$ nm, $d_2 = 10$ nm).

7. Conclusions

A photonic crystal design approach was proposed in order to predict the spectral richness and selectivity of artificial reflectors made of periodic multilayer structures. The predictions gave results consistent with rigorous reflectance spectrum calculations and observations on biological specimens. Thanks to a bio-inspired design, we showed that an artificial reflector made of $\text{SiO}_2/\text{TiO}_2$ multilayer structure was able to produce similar colors as a biological air/chitin structure. The bio-inspired novel aspect of the artificial reflector relied on the strong unbalance between the thicknesses of the two layers forming the unit cell.

Acknowledgments

This investigation was conducted with the support of the European NEST STREP BioPhot project (contract n°12915). C. Vandenberghe was supported as research fellow by the Belgian National Fund for Scientific Research (FNRS).